ISSN 1063-7788, Physics of Atomic Nuclei, 2017, Vol. 80, No. 1, pp. 60–66. © Pleiades Publishing, Ltd., 2017.
Original Russian Text © L. Zaidi, E.A. Kashaeva, S.I. Lezhnin, G.N. Malyshkin, S.I. Samarin, T.V. Sycheva, S.Yu. Taskaev, S.A. Frolov, 2017, published in Yadernaya Fizika, 2017, Vol. 80, No. 1, pp. 63–69.

ELEMENTARY PARTICLES AND FIELDS
Experiment

Neutron-Beam-Shaping Assembly for Boron Neutron-Capture Therapy

L. Zaidi[1)], E. A. Kashaeva[2)], S. I. Lezhnin[3),4)], G. N. Malyshkin[2)], S. I. Samarin[2)], T. V. Sycheva[5)], S. Yu. Taskaev[4),5)*], and S. A. Frolov[2)]

Budker Institute of Nuclear Physics, Siberian Branch, Russian Academy of Sciences, pr. Akademika Lavrentieva 11, Novosibirsk, 630090 Russia

Received January 27, 2016

Abstract—A neutron-beam-shaping assembly consisting of a moderator, a reflector, and an absorber is used to form a therapeutic neutron beam for the boron neutron-capture therapy of malignant tumors at accelerator neutron sources. A new structure of the moderator and reflector is proposed in the present article, and the results of a numerical simulation of the neutron spectrum and of the absorbed dose in a modified Snyder head phantom are presented. The application of a composite moderator and of a composite reflector and the implementation of neutron production at the proton energy of 2.3 MeV are shown to permit obtaining a high-quality therapeutic neutron beam.

DOI: 10.1134/S106377881701015X

1. INTRODUCTION

Boron neutron-capture therapy (BNCT) [1], which provides a selective destruction of tumor cells via the accumulation in them of the stable nonradioactive isotope ^{10}B and subsequent irradiation with neutrons, is promising method for the therapy of malignant tumors. Upon neutron absorption by boron, there occurs a nuclear reaction accompanied by a high energy deposition in tumor cells. The purposes of therapy require intense fluxes of epithermal neutrons—more precisely, neutrons of energy 1 to 30 keV [1]. The reaction $^7\mathrm{Li}(p,n)^7\mathrm{Be}$, which is characterized by a high yield of neutrons that have the softest energy spectrum is the most appropriate for this purpose. A neutron-beam-shaping (NBS) assembly that includes a moderator; a reflector; an absorber; and, in some cases, a filter is used to slow down neutrons. Over the past decade, when it became obvious that a lithium target can be manufactured, an NBS for the reaction $^7\mathrm{Li}(p,n)^7\mathrm{Be}$ with a 2.3- to 2.8-MeV proton beam was optimized by a number of research groups [2–10]. For a phantom where one calculates the distribution of doses, it is common practice to employ a modified Snyder head phantom [11], which is three ellipsoids inserted into each other that have compositions maximally close to the compositions of skin, bones, and brains. In calculations, use is made of relative-biological-effectiveness (RBE) values from [12], which are 1.0 for photons and 3.2 for neutrons in the case of brain tissues; the composite biological effectiveness (CBE) is 1.35. For a tumor, RBE is assumed to have the same values, while CBE is set to 3.8.

In calculating doses, the following processes are taken into account. First, there is the process involving neutron absorption by boron and resulting in the energy deposition of 2.79 MeV; in 6.1% of the cases, this energy is distributed only among the product lithium nucleus and alpha particle, while, in 93.9% of the cases, the lithium nucleus is emitted in an excited case, radiating a photon of energy 478 keV. Second, there is neutron capture by hydrogen nuclei, which leads to the formation of deuterium and the emission of 2.2-MeV photons. Third, there arise recoil protons both from the interaction of neutrons, predominantly fast ones, with matter nuclei, primarily with hydrogen, and from neutron absorption by nitrogen nuclei, which is accompanied by the energy deposition of 580 keV. The flux of photons from the target and from the beam shaper is taken into account quite frequently. The process of neutron absorption by

[1)]University of Science and Technology Houari Boumediene, BP 32 El Alia 16111, Bab Ezzouar 16111, Algeria.
[2)]Zababakhin All-Russian Scientific Research Institute for Technical Physics (VNIITF), P.O. Box 245, Snezhinsk, Chelyabinsk oblast, Russia.
[3)]Novosibirsk Branch, Nuclear Safety Institute, Russian Academy of Sciences, pr. Akademika Lavrentieva 1, Novosibirsk, 630090 Russia.
[4)]Novosibirsk State University, ul. Pirogova 2, Novosibirsk, 630090 Russia.
[5)]Budker Institute of Nuclear Physics, Siberian Branch, Russian Academy of Sciences, pr. Akademika Lavrentieva 11, Novosibirsk, 630090 Russia.
*E-mail: taskaev@inp.nsk.su

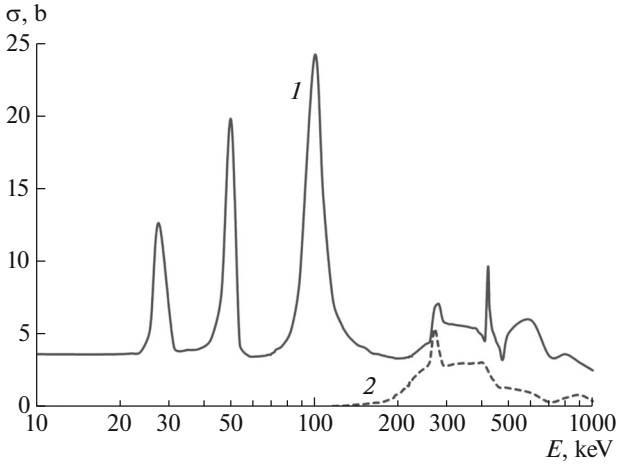

Fig. 1. Cross sections for (*1*) elastic and (*2*) inelastic neutron scattering on fluorine versus the neutron energy according to the ENDF/B-VII.1 database.

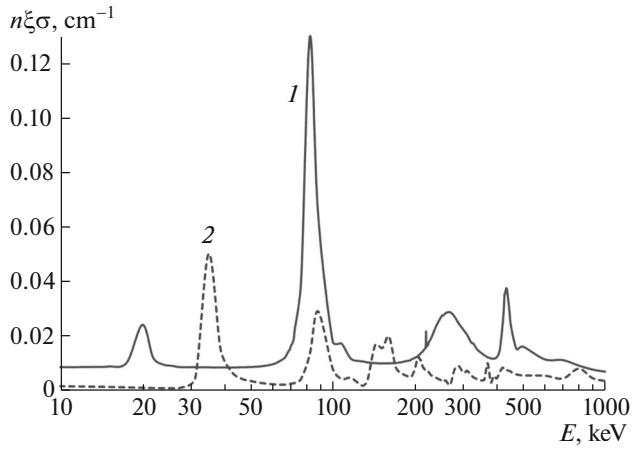

Fig. 2. Rate of neutron moderation on (*1*) magnesium and (*2*) aluminum versus the neutron energy.

chlorine is disregarded almost always because of the smallness of its cross section.

The prevalent opinion is that the moderator should contain highest concentrations of fluorine since only fluorine has a sizable cross section for inelastic neutron scattering in the energy region below 1 MeV, so that this ensures their fast moderation to energies of about 200 keV (see Fig. 1). A hydrogen-containing moderator can reduce the neutron energy efficiently, but there occurs, in this case, an overly strong shift of the resulting neutron spectrum toward thermal energies, so that it becomes inappropriate for the therapy of deeply seated tumors. Lead or graphite is used as a reflector. Polyethylene doped with boron and lithium may be an absorber. Such NBS assemblies used together with a proton beam of energy 2.5 MeV and current 10 mA provide at dose rate at a level of 1 Gy Eq./min, a therapy depth (distance from the surface to the point where the dose rate in a tumor exceeds the maximum dose rate in a sound tissue) of up to 10 cm, and a therapeutic ratio (ratio of the the maximum dose powers in a tumor and healthy cells) of up to 4. This is quite acceptable for performing boron neutron-capture therapy.

In the present study, we carry out a critical analysis of the decisions adopted previously in what concerns the structure of NBS assemblies, put forth proposals that would contribute to improving the quality of therapeutic neutron beams, and perform an optimization of NBS assemblies.

2. RESULT OF NUMERICAL CALCULATIONS AND DISCUSSION

We begin our consideration by addressing a moderator that should not only slow down neutrons to required energies but also accomplish this over a minimum thickness in order to minimize the loss of the neutron flux density. Table 1 gives information about the densities of fluorides and about the concentration of fluorine nuclei in them. One can see that the fluorine concentrations in magnesium, aluminum, and lithium fluorides are maximal and are nearly identical. In calcium fluoride and in fluoroplastic, the fluorine concentration is substantially lower; therefore, it would not be reasonable to use these materials in a moderator. Among the remaining fluorides, lithium fluoride is only considered as a thin filter at the output of NBS assemblies for absorbing thermal neutrons originating from the reaction $^6\mathrm{Li}(n,\alpha)^3\mathrm{H}$ (the cross section for thermal-neutron absorption is 940 b).

Let us consider in detail elastic neutron scattering on magnesium and aluminum. Since the mass numbers of magnesium and aluminum nuclei are close to each other, the values of the mean logarithmic energy loss in them, ξ, are also close: they are 0.08 for magnesium and 0.072 for aluminum. The rate of neutron moderation on these nuclei in fluorides is proportional to the density of nuclei, n; the scattering

Table 1. Densities of fluorides and densities of fluorine in them

	Density, g cm^{-3}	Concentration of fluorine nuclei, 10^{22} cm^{-3}
Magnesium fluoride MgF_2	3.177	6.14
Aluminum fluoride AlF_3	2.88	6.19
Lithium fluoride LiF	2.639	6.13
Calcium fluoride CaF_2	3.18	4.90
Fluoroplastic C_2F_4	2.2	5.29

Table 2. Results of calculations for various versions of the NBS assembly for a proton beam of energy 2.3-MeV and current 10-mA

	Version 1 MgF_2	Version 2 AlF_3	Version 3 $MgF_2 + AlF_3$	Version 4 $MgF_2 + AlF_3$ graphite
Epithermal-neutron flux density [10^8 cm^{-2}]	8.04	9.02	8.76	10.2
Fast-neutron flux density [10^8 cm^{-2}]	1.49	2.04	1.49	0.61
Thermal-neutron flux density [10^8 cm^{-2}]	0.22	0.21	0.21	1.96
Average neutron energy [keV]	17	19	18	7
Photon flux density [10^8 cm^{-2}]	0.37	0.51	0.42	0.62
Average photon energy [keV]	312	300	314	385
Dose rate in tumor [Gy Eq./min]	1.68	1.83	1.76	2.14
Therapeutic ratio	2.8	2.17	2.54	4.1

cross section, σ; and the mean logarithmic energy loss, ξ. We depict it Fig. 2. One can see that, nearly the whole energy range under study, with the exception of regions around 35 and 150 keV, neutron moderation is more efficient on magnesium than on aluminum. An appealing feature of aluminum is that it is nearly transparent to neutrons of energy below 30 keV.

We have considered three versions of the NBS assembly featuring a moderator $d = 20$ cm in diameter and $h = 20$ cm in height that is manufactured from (i) magnesium fluoride, (ii) aluminum fluoride, and (iii) their combination. A magnesium-fluoride cylinder 12 cm in height was the closest to the target, and an aluminum-fluoride cylinder 8 cm in height was under it. The layout of the NBS assembly is shown in Fig. 3. A moderator, a target, and a vacuum chamber are surrounded by a lead reflector of external diameter $D = 60$ cm and height $h + H = 50$ cm. The lower parts of the reflector and moderator are positioned at the same altitude. The whole reflector, with the exception of its lower part, is surrounded by a polyethylene absorber featuring a 7.5% addition of natural lithium 5 cm thick. A modified Snyder head phantom was placed on the axis 5 cm below the moderator. The proton energy was 2.3 MeV, and the proton-beam current and diameter were 10 mA and 100 mm, respectively. In our calculations, the neutron-producing target was taken in the form of disks 100 mm in diameter from lithium (100 μm thick), tantalum (0.4 mm thick), water (2 mm thick), tantalum (0.4 mm thick) and copper (3 mm thick). A numerical simulation of proton, neutron, and gamma-radiation transport was performed by the Monte Carlo method with the aid of PRIZMA code [13] and the ENDF/B-VI database of neutron and gamma-ray interactions with matter [14]. In order to describe the nuclear interaction of protons with a lithium target, data on the reaction $^7\mathrm{Li}(p,n)^7\mathrm{Be}$ producing neutrons and the reaction $^7\mathrm{Li}(p,\gamma)^8\mathrm{Be} \to 2\alpha$ appearing to be a source of high-energy gamma rays were taken from [15], while data on the gamma-ray-generating reaction $^7\mathrm{Li}(p,p')^{7(1*)}\mathrm{Li}$ were prepared on the basis of the EXFOR database [16]. The concentration of ^{10}B was set to 15 ppm in sound tissues and to 52.5 ppm in a tumor. The results of the calculations are given in

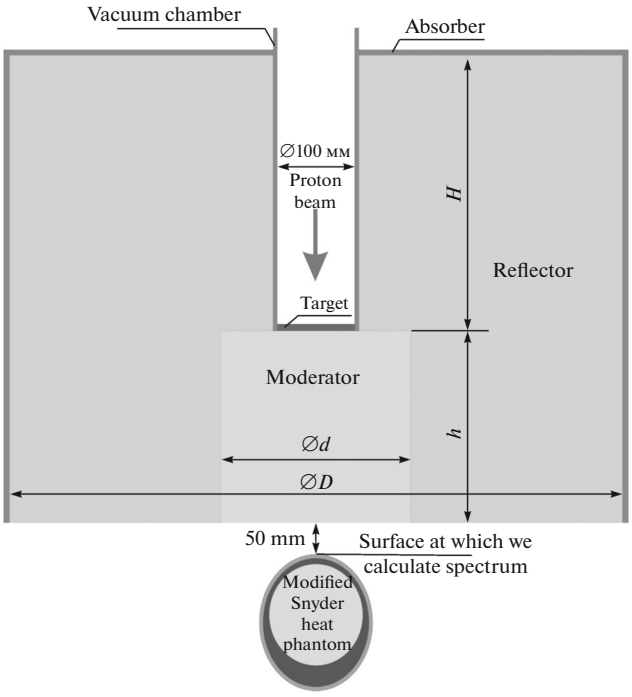

Fig. 3. Beam-shaper geometry and position of a modified Snyder head phantom.

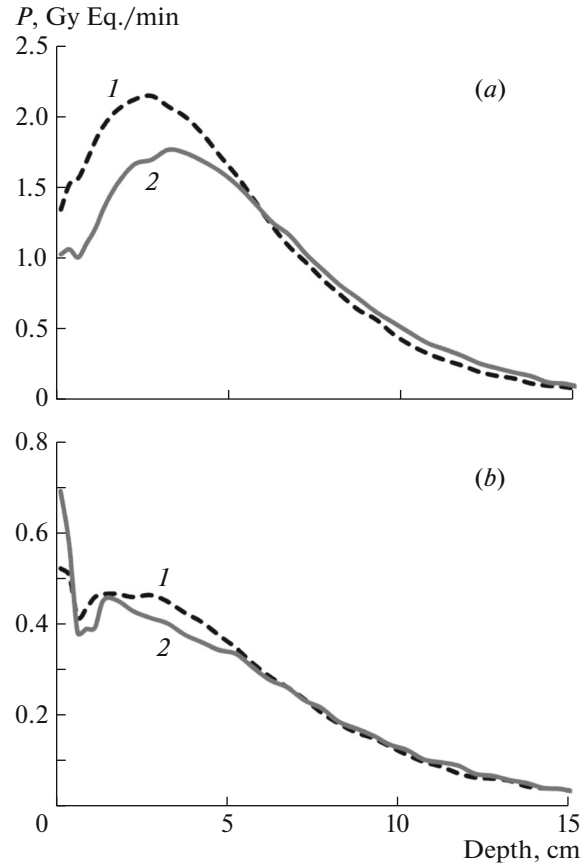

Fig. 4. Distribution of the dose rate over the depth in the (*a*) tumor and (*b*) sound tissue for the case of employing (*1*) graphite and (*2*) lead reflectors in the forward hemisphere.

Table 2 (here, the boundary between the epithermal- and fast-neutron ranges is shifted from 10 to 30 keV, which is the upper boundary of the spectrum of optimal neutrons for boron neutron-capture therapy. As might have been expected, a magnesium-fluoride moderator as considered in relation to an aluminum fluoride moderator yields a softer spectrum, a fast-neutron flux lower by a factor of 1.37, and a therapeutic ratio better by a factor of 1.3, but an epithermal-neutron flux lower by a factor of 1.12, so that the dose rate in tumors appears to be lower. As a matter of fact, a combination of fluorides in an NBS assembly makes it possible to have advantages of each of them within a single scheme: the epithermal-neutron flux density is nearly as large (only 3% smaller) as that in the case of applying aluminum fluoride), and the fast-neutron flux is low, as in the case of applying magnesium fluoride alone. Thus, an optimum solution would be to fabricate a composite moderator consisting of magnesium fluoride positioned closer to the target and aluminum fluoride placed closer to the output.

The next proposal for revising the solutions adopted earlier concerns the reflector. Neutrons produced in the forward direction have a substantially higher energy than those that go in the backward direction [17]. Therefore, we propose to apply, in the forward hemisphere, a graphite reflector, in which case the moderation of neutrons accompanies their reflection ($\xi = 0.158$), and, in the backward hemisphere, a lead absorber without antimony admixtures, where neutron reflection occurs nearly without a loss of energy ($\xi = 0.01$). In Table 2, the results of the calculation for an NBS assembly featuring such a graphite reflector in the forward hemisphere are given in the Version 4 column. One can see that the energy spectrum of neutrons became softer and that the epithermal-neutron flux density grew; this led to an increase in the dose rate in the tumor and in the therapeutic ratio. Figure 4 shows the distribution of the dose rate over the depth in the tumor and in the sound tissue. One can see that a graphite reflector in the forward hemisphere makes it possible to obtain a substantially higher radiation depth in tumors seated at a depth of up to 6 cm. In the case of deeper seated tumors, the use of lead reflector ensures higher radiation doses.

We now proceed to optimize the dimensions of NBS assemblies. The respective calculations were performed by means of the NMC code, which was intended for simulating neutron transport in three dimensions by the Monte Carlo method with the aid of the ENDF-VII cross-section database. The structure of the code was described in [18, 19]. In Table 3, the results obtained by calculating the radiation dose (P) and the therapeutic ratio (AR) for a moderator from magnesium fluoride of various height h and diameter d at the proton-beam energies of 2.5 and 2.3 MeV are shown for the cases of a lead or a graphite reflector $D = 60$ cm in diameter. The following dimensions of the moderator seem optimal (the respective cells in Table 3 are gray): at the energy of 2.5 MeV, the diameter and height are both 30 cm, while, at the energy of 2.3 MeV, the diameter and height are 30 and 25 cm, respectively, in the case of a lead reflector and are both 20 cm in the case of a graphite reflector in the forward hemisphere.

For a NBS assembly featuring a magnesium-fluoride absorber $d = 20$ cm in diameter and $h =$ 20 cm in height and operating with a proton beam of energy 2.3 MeV and current 10 mA, the radiation dose and the therapeutic ratio are determined for the case where there is a graphite reflector in the forward hemisphere and where its diameter D changes from 0 to 140 cm with a step of 20 cm. As the reflector diameter becomes larger, the dose rate grows and reaches a plateau rather quickly. For example, it is 74%, 93%, and 97% of the maximum dose rate at the reflector-diameter values of $D = 40$, 60, and 80 cm, respectively. The use of a reflector 80 cm in

diameter seems optimal. We note that, in the absence of a reflector, the dose rate diminishes to 11% of the maximum value. This suggests that a major part of neutrons escapes from the moderator and returns back after the interaction with the reflector.

In a similar way, we have determined the radiation rate at various values of the height H of the lead reflector in the backward hemisphere that change from 0 to 100 cm with a step of 10 cm. As the reflector height becomes larger, the radiation rate grows and also reaches a plateau rather quickly. For example, it is 96% and 99% of the maximum value at the heights of $H = 20$ cm and $H = 30$ cm, respectively. In the absence of a lead absorber in the backward hemisphere, the dose rate falls down to a value of 53%.

We now proceed to consider the problem of determining an optimum energy of the proton beam. The cross section for the reaction $^7\mathrm{Li}(p,n)^7\mathrm{Be}$ is given in Fig. 5. For the purposes of boron neutron-capture therapy, one usually considers proton beams of energy 2.5 to 2.8 MeV, in which case the neutron yield is quite large. We propose employing a proton beam of energy 2.3 MeV, which is close to that at which the cross section for the above reaction reaches a maximum. As the proton energy grows above 2.3 MeV, the neutron yield increases, of course, but at a lower rate than at lower energies; moreover, these additional neutrons will have a higher energy.

By way of example, we indicate that, for an NBS assembly consisting of a magnesium-fluoride moderator $h = 21$ cm in height and $d = 20$ cm in diameter and a reflector $D = 80$ cm in diameter, an increase in the proton energy from 2.3 to 2.5 MeV leads to an increase in the neutron-flux density by a factor of 1.75—owing primarily to more energetic neutrons (see Fig. 6)—and, as a consequence, to a growth of the dose rate in tumors nearly in the same proportion.

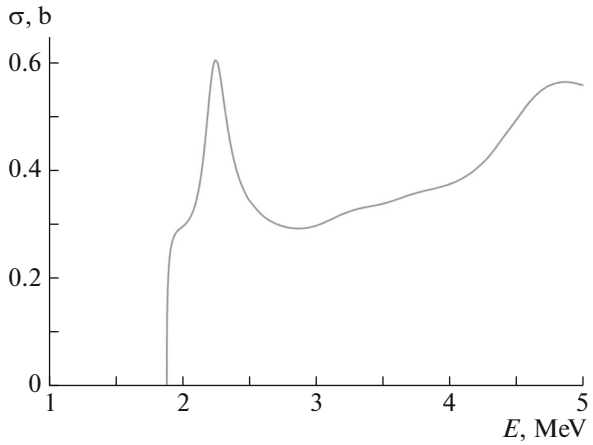

Fig. 5. Cross section for the reaction $^7\mathrm{Li}(p,n)^7\mathrm{Be}$ as a function of the proton energy according to the ENDF/B-VII.1 database.

However, the appearance of a sizable fast-neutron component (especially in the region between 250 keV and 1 MeV) leads to the growth of the dose rate in sound cells at the surface by a factor of 2.56, with the result that the therapeutic ratio decreases from 5.4 to 3.7. In order to reduce the effect of fast neutrons, it is necessary to increase the moderator height. Upon the increase in this height from 21 to 26 cm, the fast-neutron effect becomes weaker to such an extent that the therapeutic ratio reaches nearly the same value, 5, but, concurrently, the dose rate decreases by a factor of 1.6. Figure 6 shows that the neutron spectra become similar, and there is no use in increasing the proton energy. Moreover, the spectrum of neutrons generated at the proton energy of 2.5 MeV involves a sizable flux of neutrons whose energies are above 500 keV, since the moderation efficiency for them is insufficient. Table 4 gives the calculated energy loss of a neutron inelastically scattered on fluorine. One can see that, at an initial energy in the range between 200 and 400 keV, an inelastically scattered neutron loses 50% of its energy, while, at initial energies in excess of 500 keV, the respective energy loss is 30%.

Thus, therapeutic neutron beams of best quality are obtained upon employing a proton beam of energy 2.3 MeV or energy close to it. The use of a higher energy proton beam may justified only for tumors seated at a depth in excess of 7 cm. In that case, it is desired to generate harder neutrons in order that they penetrate deeper into tissues and to seek a solution to the problem of reducing the dose rate in healthy cells at the surface by directing a beam from different sides

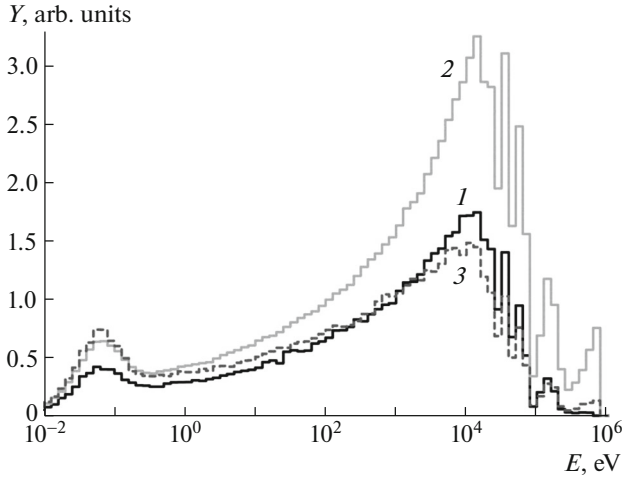

Fig. 6. Energy spectrum of the shaped neutron beam at (*1*) the proton-beam energy of 2.3 MeV and the moderator height of 21 cm, (*2*) the proton-beam energy of 2.5 MeV and the moderator height of 21 cm, and (*3*) the proton-beam energy of 2.5 MeV and the moderator height of 26 cm.

Table 3. Optimization of the moderator height and diameter

d, cm	h, cm	2.5 MeV, Pb		2.3 MeV, Pb		2.3 MeV, graphite	
		P, Gy Eq./min	AR	P, Gy Eq./min	AR	P, Gy Eq./min	AR
30	40	1.2	4.6				
	35	1.6	4.8				
	30	2.3	5.2	1.4	5.4		
	25	3.1	4.8	1.8	5.3	1.6	5.3
	20	4.4	3.3	2.5	4.8	2.2	5.3
	15	6.6	1.9	2.9	4.8	3.2	3.7
	10	12.4	1.2				
20	30			1.3	4.7		
	25			1.8	4.2		
	20			2.4	3.3	2.2	5.2
	15			3.5	2.4		
40	20					2.2	5.2
50	20					2.1	5.3
60	20					2.1	5.3

Table 4. Energy loss of neutrons scattered inelastically on fluorine

Initial neutron energy [keV]	200	300	400	500	600	700	800	900	1000
Neutron energy loss [keV]	123	153	210	205	225	243	225	260	261

with the aid of a rotatable orthogonal neutron-beam shaper [20, 21].

3. CONCLUSIONS

A neutron-beam-shaping assembly consisting of a moderator, a reflector, and an absorber is used at accelerator neutron sources to obtain a therapeutic neutron beam for the boron neutron-capture therapy of malignant tumors. For the first time, we have proposed here employing a composite moderator formed by magnesium fluoride near the neutron-producing target and aluminum fluoride near the output along with a composite reflector from graphite in the forward hemisphere and lead in the backward hemisphere and generating neutrons via the reaction $^7\mathrm{Li}(p,n)^7\mathrm{Be}$ induced by 2.3-MeV proton beam. By means of a numerical simulation of neutron and gamma-radiation transport, we have shown that the proposed solutions make it possible to shape a therapeutic neutron beam meeting to a great extent the requirements of boron neutron-capture therapy.

ACKNOWLEDGMENTS

This work was funded by the Russian Science Foundation under project no. 14-32-00006 and was supported by Budker Institute of Nuclear Physics (Siberian Division, Russian Academy of Sciences).

REFERENCES

1. *Neutron Capture Therapy: Principles and Applications*, Ed. by W. Sauerwein, A. Wittig, R. Moss, and Y. Nakagawa (Springer, Berlin, 2012).
2. F. Palamara, F. Mattioda, R. Varone, and V. Guisti, in *Research and Development in Neutron Capture Therapy*, Ed. by W. Sauerwein, R. Moss, and A. Wittig (Monduzzi Editore, Bologna, Italy, 2002), p. 283.

3. A. Hawk, T. Blue, J. Woolard, and G. Gupta, in *Research and Development in Neutron Capture Therapy*, Ed. by W. Sauerwein, R. Moss, and A. Wittig (Monduzzi Editore, Bologna, Italy, 2002), p. 253.
4. O. E. Kononov, V. N. Kononov, M. V. Bokhovko, et al., Appl. Radiat. Isot. **61**, 1009 (2004).
5. G. Bengua, T. Kobayashi, K. Tanaka, and Y. Nakagawa, Appl. Radiat. Isot. **61**, 1003 (2004).
6. F. Stichelbaut, E. Forton, and Y. Jongen, in *Proceedings of the 12th International Congress on Advances in Neutron Capture Therapy, Takamatsu, Japan, Oct. 9–13, 2006,* p. 308.
7. K. Tanaka, T. Kobayashi, G. Bengua, et al., in *Proceedings of the 12th International Congress on Advances in Neutron Capture Therapy, Takamatsu, Japan, Oct. 9–13, 2006,* p. 323.
8. R. Terlizzi, N. Colonna, P. Colangelo, et al., Appl. Radiat. Isot. **67**, S292 (2009).
9. D. M. Minsky, A. J. Kreiner, and A. A. Valda, Appl. Radiat. Isot. **69**, 1668 (2011).
10. A. A. Burlon et al., Appl. Radiat. Isot. **69**, 1688 (2011).
11. J. T. Goorley, W. S. Kiger III, and R. G. Zamenhof, Med. Phys. **29**, 145 (2002).
12. O. K. Harling and K. J. Riley, J. Neuro-Oncol. **62**, 7 (2003).
13. Y. Z. Kandiev et al., Ann. Nucl. Energy **82**, 116 (2015).
14. https://www-nds.iaea.org/exfor/endf.htm.
15. S. N. Abramovich et al., *Nuclear-Physics Constants of Thermonuclear Fusion: Reference Book* (TsNIIatominform, Moscow, 1989) [in Russian].
16. https://www-nds.iaea.org/exfor/exfor.htm.
17. C. L. Lee and X.-L. Zhou, Nucl. Instrum. Methods Phys. Res. B **152**, 11 (1999).
18. D. V. Yurov et al., Fusion Eng. Des. **87**, 1684 (2012).
19. S. A. Brednikhin, S. I. Lezhnin, S. A. Frolov, and D. V. Yurov, NSI RAS Preprint No. 2012-04 (Nucl. Safety Inst., RAS, Moscow, 2012).
20. V. V. Kanygin and C. Yu. Taskaev, RF Patent No. 2540124 (2014).
21. V. Aleynik et al., Appl. Radiat. Isot. **88**, 177 (2014).